expect TlR compounds with organic groups R such as CF_3 or $CH(CO_2Me)_2$, which are able to accommodate negative charge to be more stable than those with, e.g., R= CH_3 or Ph.

(e) Tl-Tl bonds are very weak or do not exist because of spin-orbit coupling and inert pair effects. The only reported species with a stable Tl-Tl bond, $Tl_2Me_6^{2-}$, is doubtful in our opinion. The compounds M_2Me_6 (M = Sn, Pb), isoelectronic with $Tl_2Me_6^{2-}$, are known to form stable metal-metal bonds, but they are measured to be less stable than the simple metal dimers M_2.[38,44,56,87] The reason could be an electrostatic repulsion in the $R_3M^{\delta+}-^{\delta+}MR_3$ compounds in contrast to M_2. The same argument holds for $Tl_2Me_6^{2-}$, so we expect the Tl-Tl bond to be less stable in $Tl_2Me_6^{2-}$ than in Tl_2; for the latter, the bond stability is assumed to be about 20-50 kJ/mol.

(f) The pseudopotential approximation ([Pt] core for Tl and [Ar3d^{10}] core for Br) is accurate enough to provide results that are in good agreement with experiment. The [Pt]-core definition is sufficient for calculations on organothallium compounds. The Tl(5d) participation to Tl-C σ-bonds is found to be small, as indicated by our SCF-SW-Xα results.

There have been few developments in organothallium chemistry during the last decade. Our results suggest that monoalkylthallium compounds could be generated and studied spectroscopically under certain conditions. Vibrational analyses of these compounds using the calculated SCF force field partially listed here will be published soon.

Acknowledgment. P.S. is very grateful to the Alexander von Humboldt-Stiftung for the award of a Feodor-Lynen Fellowship and financial support. Thanks are due to Mrs. Fischer (RUS Computer Center, Universität Stuttgart) for her excellent service in making possible the time-consuming jobs on the CRAY1M. We are also grateful to Dr. U. Wedig (Max-Planck Institut Stuttgart) for changing the program MELD, to Prof. H. Preuss, M. Dolg, G. Igel-Mann, H. Hayd, and K. Vogel (Universität Stuttgart) for their interest and assistance in performing part of these calculations at the University of Stuttgart, to Dr. A. J. Downs (University Oxford) for allowing us to quote results of unpublished work, and to Prof. G. M. Sheldrick (Universität Göttingen) for some helpful suggestions. We also express our gratitude to Prof. M. J. Taylor (University Auckland) and Prof. W. H. E. Schwarz (Universität Siegen) for valuable discussions and for critically reading this paper.

Registry No. TlH, 13763-69-4; TlH_2, 117439-42-6; TlH_3, 82391-14-8; TlH_4^-, 58220-54-5; TlH_2^+, 117470-02-7; $TlCH_3^+$, 117470-03-8; $TlCH_3$, 82391-13-7; TlC_2H_3, 117439-43-7; TlC_2H, 117439-44-8; $Tl(CH_3)_2$, 117439-45-9; $Tl(CH_3)_2^+$, 16785-98-1; $Tl(CH_3)_2Br$, 21648-59-9; $Tl(CH_3)_3$, 3003-15-4; $Tl(CH_3)_4^-$, 117470-04-9.

(87) (a) Lappert, M. F.; Pedley, J. B.; Simpson, J.; Spalding, T. R. *J. Organomet. Chem.* **1971**, *29*, 195. (b) Davies, J. V.; Pope, A. E.; Skinner, H. A. *Trans. Faraday Soc.* **1963**, *59*, 2233.

Hydrogen Bonding and Proton Transfers Involving the Carboxylate Group

Sławomir M. Cybulski and Steve Scheiner*

Contribution from the Department of Chemistry & Biochemistry, Southern Illinois University, Carbondale, Illinois 62901-4409. *Received April 18, 1988*

Abstract: The complex formed between $HCOO^-$ and HOH is examined by ab initio methods using a 4-31+G* basis set. A number of minima are located in the potential energy surface, the most stable of which is of C_{2v} geometry wherein both protons of HOH participate in H bonds. The barrier impeding proton transfer between OH^- and $HCOO^-$ rises with increasing intermolecular separation for each of the arrangements studied. As the OH^- anion moves toward the C-O axis of $HCOO^-$, the equilibrium position of the bridging proton is shifted toward the former group, paralleling earlier observations for the pair of neutral subunits HCOOH and HOH. On the other hand, $HCOO^-$ and HCOOH behave in different fashion with respect to motions of the hydroxyl group out of the carboxyl plane. These patterns are explained simply on the basis of differing ion-dipole interactions, as are small differences in the optimal geometries and proton-transfer behavior of the various arrangements of the two subunits.

I. Introduction

Since proton transfers comprise perhaps the simplest and most common reaction in chemistry, research into this process has led to a truly enormous body of literature over the years.[1] Most of the early work was limited to study of the reaction in solution, making it difficult to extract properties that are intrinsic to the transfer itself from complications arising from solvent effects. Modern developments have allowed the process to be studied in the gas phase, leading to important advances in our understanding of the phenomenon.[2] Because theoretical calculations are most easily carried out for a given system in isolation, ab initio methods have also made some contributions to this field.[3] The calculations have been especially helpful in providing information that is not readily obtained from experiment, e.g. geometries of short-lived species.

In an effort to achieve a comprehensive understanding of the principles underlying proton-transfer reactions, ab initio methods have been applied systematically in this laboratory to a variety of different systems.[4-7] Calculations of very small and simple

(1) For some summaries, see: Caldin, E. F., Gold, V., Eds. *Proton-Transfer Reactions*; Chapman and Hall: London, 1975. Stewart, R. *The Proton: Applications to Organic Chemistry*; Academic: Orlando, FL, 1985. Kresge, A. J. *Acc. Chem. Res.* **1975**, *8*, 354. Koch, H. F. *Ibid.* **1984**, *17*, 137.

(2) Larson, J. W.; McMahon, T. B. *J. Phys. Chem.* **1987**, *91*, 554. Fuke, K.; Yabe, T.; Chiba, N.; Kohida, T.; Kaya, K. *Ibid.* **1986**, *90*, 2309. Han, C.-C.; Dodd, J. A.; Brauman, J. I. *Ibid.* **1986**, *90*, 471. Farneth, W. E.; Brauman, J. I. *J. Am. Chem. Soc.* **1976**, *98*, 7891. Hierl, P. M.; Ahrens, A. F.; Henchman, M.; Viggiano, A. A.; Paulson, J. F. *J. Am. Chem. Soc.* **1986**, *108*, 3140.

(3) Siria, J. C.; Duran, M.; Lledos, A.; Bertran, J. *J. Am. Chem. Soc.* **1987**, *109*, 7623. Dijkman, J. P.; Osman, R.; Weinstein, H. *Int. J. Quantum Chem., Quantum Biol. Symp.* **1987**, *14*, 211. Jasien, P. G.; Stevens, W. J. *Chem. Phys. Lett.* **1986**, *130*, 127. Basch, H.; Krauss, M.; Stevens, W. J. *J. Am. Chem. Soc.* **1985**, *107*, 7267. McKee, M. L. *J. Am. Chem. Soc.* **1987**, *109*, 559. Cao, H. Z.; Allavena, M.; Tapia, O.; Evleth, E. M. *J. Phys. Chem.* **1985**, *89*, 1581. Alagona, G.; Desmeules, P.; Ghio, C.; Kollman, P. A. *J. Am. Chem. Soc.* **1984**, *106*, 3623.

(4) Scheiner, S. *J. Am. Chem. Soc.* **1981**, *103*, 315.

(5) Scheiner, S. *Acc. Chem. Res.* **1985**, *18*, 174. Hillenbrand, E. A.; Scheiner, S. *J. Am. Chem. Soc.* **1985**, *107*, 7690. Scheiner, S.; Redfern, P. *J. Phys. Chem.* **1986**, *90*, 2969. Cybulski, S. M.; Scheiner, S. *J. Am. Chem. Soc.* **1987**, *109*, 4199.

(6) Scheiner, S.; Hillenbrand, E. A. *J. Phys. Chem.* **1985**, *89*, 3053. Scheiner, S.; Hillenbrand, E. A. *Proc. Natl. Acad. Sci. U.S.A.* **1985**, *82*, 2741.

0002-7863/89/1511-0023$01.50/0 © 1989 American Chemical Society

Table I. Geometries Optimized at the SCF Level[a]

	HOH	OH^-
r(OH)	0.948	0.953
θ(HOH)	106.6	
E^{SCF}, au	−75.94863	−75.30886
E^{MP2}, au	−76.14277	−75.52490

	HCOOH(C)	HCOOH(T)	$HCOO^-$
r(HC)	1.088	1.082	1.117
r(CO′)	1.327	1.321	1.233
r(CO″)	1.175	1.182	1.233
r(O′H)	0.949	0.954	
θ(HCO′)	114.0	110.6	114.7
θ(HCO″)	123.1	124.6	114.7
θ(CO′H)	112.2	109.9	
E^{SCF}, au	−188.58399	−188.59355	−188.03332
E^{MP2}, au	−189.08085	−189.08971	−189.54555

[a] O′ is hydroxyl oxygen of HCOOH, and O″ represents the carbonyl oxygen. C and T indicate whether two H atoms of HCOOH are cis or trans to one another. Distances are in angstroms and angles in degrees.

systems such as $(H_2O{\cdot}H{\cdot}OH_2)^+$ led to identification of a number of proton-transfer properties intrinsic to the oxygen atom.[4,5] When H_2O was replaced with H_2CO, it was possible to derive the fundamental differences between the behavior of a hydroxyl and carbonyl oxygen, i.e. single- vs double-bonded.[6] Placing both types of oxygen on the same group yields the carboxyl moiety; study of −COOH provided information on the manner in which the two O atoms influence one another's behavior.[7] As an example of one principle that has emerged from previous calculations, it has been demonstrated that, as the partner subunit is moved toward a position collinear with the C–O bond, there is a marked propensity of the bridging proton to move away from the −COOH and toward the proton acceptor.

Most of our earlier work has dealt with proton-bound dimers of neutral subunits. For instance, the carboxyl group was studied[7] by constructing a H-bonded system of HCOOH, a proton, and HOH as a proton acceptor group: $(HC(OH)O{\cdot}H{\cdot}OH_2)^+$. However, the $-COO^-$ anion figures prominently in a diversity of chemical systems. The carboxylate group of Asp and Glu residues of proteins, which plays a major role in the mechanism of a large number of enzymes,[8] is a case in point. For that reason, we turn our attention here to the proton-transfer properties of the $-COO^-$ anion.

In analogy with the previous study of neutral HCOOH, which was paired with neutral HOH as proton acceptor,[7] the present system is constructed by coupling $HCOO^-$ with OH^- as acceptor: $(HCOO{\cdot}H{\cdot}OH)^-$. Comparison of the results obtained with the latter system and the earlier data for $(HC(OH)O{\cdot}H{\cdot}OH_2)^+$ will allow us to draw conclusions concerning the effect of charge state on the proton-transfer properties of the carboxyl group. The results should find immediate application to the functioning of enzymes in which either a −COOH or $-COO^-$ group may be involved in the mechanism.

Following a description of the theoretical method and justification for its choice in the next section, we discuss the various conformations of the $(HCOO{\cdot}H{\cdot}OH)^-$ complex and the salient features of their optimized geometries. Section IV describes the effect on the proton-transfer potential of varying the distance between the two subunits. Angular deformations of the H bond, which have been shown in the past to produce striking changes in the transfer potentials, are discussed in the succeeding section, followed by a summary and listing of our principal conclusions.

II. Choice of Method

All calculations were carried out with the ab initio GAUSSIAN 80 and GAUSSIAN 82 programs.[9] Geometries were optimized via the gradient schemes contained therein or with the GAUSSIAN-compatible code developed by Baker.[10] Vibrational frequencies were calculated according to the analytical second-derivative technique of GAUSSIAN 82.

Table II. Proton Affinities (kcal/mol)[a]

	ΔE^{elec}		ΔZPE[b]	ΔH(298 K)		
	SCF	MP2	SCF	SCF	MP2	expt[c]
OH^-	401.3	386.3	8.68	393.8	378.8	391.3
$HCOO^-$	351.5	340.4	9.18	343.7	332.6	345.2

[a] All geometries were optimized at the SCF level. Calculated results corrected by counterpoise procedure with corrections as follows. SCF level: OH^-, 0.20; $HCOO^-$, 0.09. SCF + MP2 level: OH^-, 1.40; $HCOO^-$, 1.03. [b] Difference in zero-point vibrational energy between indicated anion and corresponding protonated neutral. [c] From ref 13.

Whereas our previous calculations[7] of the proton-bound dimer of HCOOH with OH_2 were able to make good use of the 4-31G* basis set,[11] the anionic $HCOO^-$ and OH^- subunits of the present system require a somewhat more flexible set. We therefore added to the standard 4-31G* set (with six Cartesian d functions) an additional diffuse sp function on C (α_{sp} = 0.04) and on O (α_{sp} = 0.068). This basis set is denoted herein as 4-31+G*.[12]

As a primary test of the suitability of this basis set for examination of proton transfer between $HCOO^-$ and OH^-, the proton affinities of these two anions were calculated. Table I reports the fully optimized geometries of these anions and the neutral molecules resulting from their protonation. Note that the T structure of HCOOH, in which the two hydrogens are trans to one another, is more stable than the C (cis) conformer. The difference in energy between the neutral and corresponding anion represents the electronic contribution to the proton affinity, reported in the first two columns of Table II. Each value has been corrected for basis set superposition error by the counterpoise procedure.[14] These corrections were negligible (less than 0.2 kcal/mol) at the SCF level but somewhat larger (between 1.0 and 1.4 kcal/mol) at the MP2 level. Note that correlation effects lower the proton affinities of the two anions by between 11 and 15 kcal/mol, consistent with the reduction observed in other systems previously.[15] At either the SCF or MP2 level, a proton is found to bind considerably more tightly to OH^- than to $HCOO^-$.

The values reported for ΔH(298 K) in Table II have been adjusted by the standard thermodynamic formulae for translational, rotational, and vibrational degrees of freedom.[16] The largest correction is due to zero-point vibrational energies, which were evaluated upon the basis of the SCF frequencies; values are listed in Table II. Comparison with the experimental values[13] in the last column suggests that our calculated proton affinities are somewhat too low. This underestimate is not entirely surprising in view of the limited size of the basis set. Moreover, extension of the Møller–Plesset expansion beyond MP2 would be expected to enlarge the proton affinity, on the basis of prior observations.[15]

But most importantly, the *difference* in calculated proton affinity between OH^- and $HCOO^-$ is 46.2 kcal/mol at the MP2 level, nearly precisely matching the experimental difference of 46.1. This difference is of paramount importance because it reflects the *relative* attraction of a proton toward the two subunits, a prime factor in studying the pro-

(7) Hillenbrand, E. A.; Scheiner, S. *J. Am. Chem. Soc.* **1986**, *108*, 7178.
(8) Hartsuck, J. A.; Lipscomb, W. N. In *The Enzymes*; Boyer, P. D., Ed.; Academic: New York, 1971; Vol. 3, pp 1–56. Sugimoto, T.; Kaiser, E. T. *J. Am. Chem. Soc.* **1979**, *101*, 3946. Knowles, J. R.; Albery, W. J. *Acc. Chem. Res.* **1977**, *10*, 105. Stroud, R. M.; Kay, L. M.; Dickerson, R. E. *J. Mol. Biol.* **1974**, *83*, 185. Matthews, D. A.; Alden, R. A.; Birktoft, J. J.; Freer, S. T.; Kraut, J. *J. Biol. Chem.* **1977**, *252*, 8875.
(9) Binkley, J. S.; Whiteside, R. A.; Krishnan, R.; Seeger, R.; DeFrees, D. J.; Schlegel, H. B.; Topiol, S.; Kahn, L. R.; Pople, J. A. *QCPE* **1981**, *13*, 406. Binkley, J. S.; Frisch, M. J.; DeFrees, D. J.; Raghavachari, K.; Whiteside, R. A.; Schlegel, H. B.; Fluder, E. M.; Pople, J. A. GAUSSIAN 82; Carnegie-Mellon University: Pittsburgh, PA, 1982.
(10) Baker, J. *J. Comput. Chem.* **1986**, *4*, 385.
(11) Ditchfield, R.; Hehre, W. J.; Pople, J. A. *J. Chem. Phys.* **1971**, *54*, 724. Hehre, W. J.; Ditchfield, R.; Pople, J. A. *Ibid.* **1972**, *56*, 2257. Collins, J. B.; Schleyer, P. v. R.; Binkley, J. S.; Pople, J. A. *J. Phys. Chem.* **1982**, *86*, 1529.
(12) These exponents differ somewhat from the "standard" values of 0.0438 and 0.0845, respectively. (Strictly speaking, 4-31+G* has no standard exponents; the values above are defined for 6-31+G*.)
(13) Bartmess, J. E.; McIver, R. T., Jr. In *Gas Phase Ion Chemistry*; Bowers, M. T., Ed.; Academic: New York, 1979; Vol. 2, pp 53–121.
(14) Boys, S. F.; Bernardi, F. *Mol. Phys.* **1970**, *19*, 553.
(15) Del Bene, J. E. *Chem. Phys. Lett.* **1983**, *94*, 213. Siggel, M. R. F.; Thomas, T. D.; Saethre, L. J. *J. Am. Chem. Soc.* **1988**, *110*, 91. DeFrees, D. J.; McLean, A. D. *J. Comput. Chem.* **1986**, *7*, 321. Ewig, C. S.; Van Wazer, J. R. *J. Phys. Chem.* **1986**, *90*, 4360. Chandrasekhar, J.; Andrade, J. G.; Schleyer, P. v. R. *J. Am. Chem. Soc.* **1981**, *103*, 5609. Mo, O.; de Paz, J. L. G.; Yanez, M. *J. Phys. Chem.* **1987**, *91*, 6484. Latajka, Z.; Scheiner, S. *Chem. Phys.* **1985**, *98*, 59. Latajka, Z.; Scheiner, S. *J. Chem. Phys.* **1984**, *81*, 2713.
(16) Levine, I. N. *Physical Chemistry*, 3rd ed.; McGraw-Hill: New York, 1988.

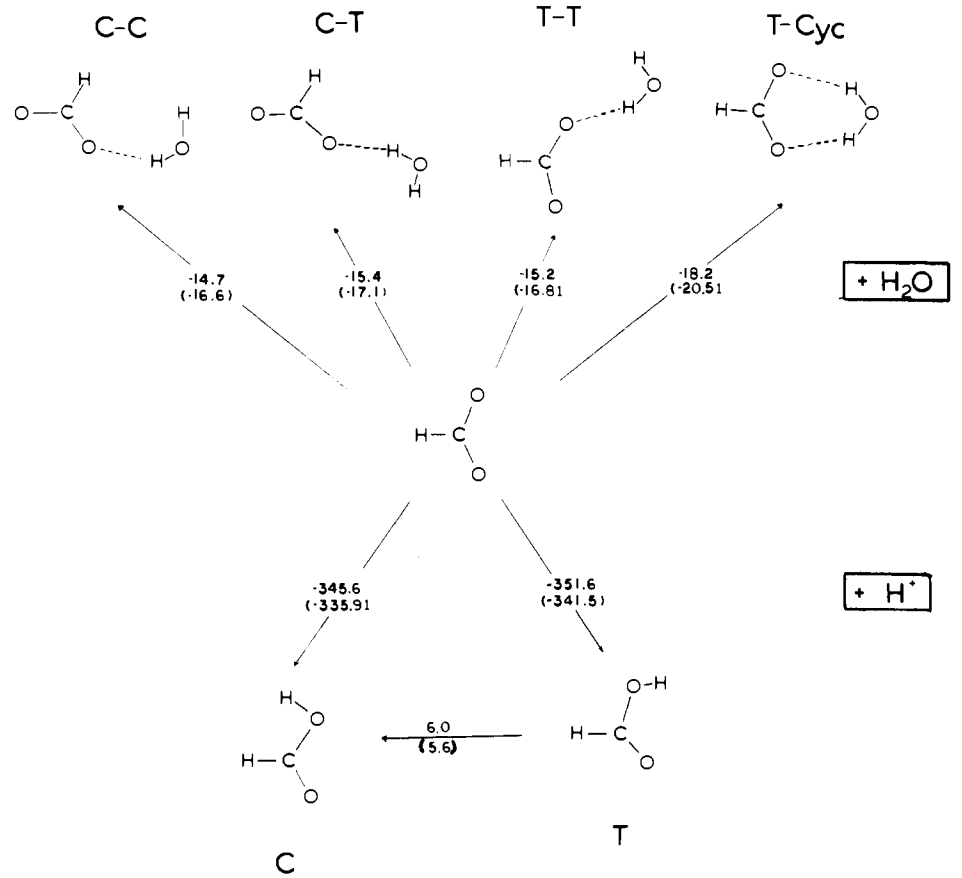

Figure 1. Pathways for hydration and protonation of $HCOO^-$, including labels used to designate each configuration. SCF energetics (kcal/mol) of each process are indicated alongside the appropriate arrows (MP2 values in parentheses). These energies do not include counterpoise corrections or zero-point vibrational contributions.

ton-transfer process. The difference in SCF proton affinities is 4 kcal/mol higher, indicating a slight bias of the proton toward OH^- at this level. The 4-31+G* basis set thus seems quite appropriate for our purposes. The experimental proton affinity difference between the two subunits is reproduced extremely well. Previous work has demonstrated that the motion of the proton induces large-scale migrations of electron density and strong changes in the nature of the interaction.[17] It is therefore a requisite also that the basis set provide a sufficiently flexible framework for correct description of electronic rearrangements that accompany the proton transfer. The diffuse sp shells and polarization functions included in 4-31+G* are expected to fulfill this criterion.

III. Optimized Structures

Since there are a number of potentially stable configurations of the proton-bound complex of $HCOO^-$ and OH^-, we introduce a shorthand notation for describing the essential features of each. This notation is designed to be consistent with our previous treatment of the complex containing the neutral HCOOH and HOH subunits where the C–H bond of HCOOH was used as a convenient reference.[7] Beginning with the $HCOO^-$ anion in the center of Figure 1, a proton may be added to an oxygen atom in a position either cis (C) or trans (T) to the C–H bond. As illustrated in the bottom half of the figure, the latter structure is calculated to be more stable than the cis configuration by 6.0 kcal/mol.

When a HOH molecule rather than H^+ is added to $HCOO^-$, the same general scheme is used to designate the position of the water. More specifically, the position of the water's O atom, cis or trans to the C–H bond of $HCOO^-$, is indicated by the first letter of each label in the upper half of Figure 1. Since the H atom of the water that participates in the H bond lies fairly close to the O···O axis (see below), its position is already known, at least to a first approximation. More useful is the position of the other H atom of water, which may lie on either side of the O···O axis; i.e., the dihedral angle ϕ(HO···OC) may be either 0° or 180°. In the first case, C is used for the second letter of each label in Figure 1 to indicate the H atom is cis to the carbon atom whereas T is used if this H atom is trans.

Complete geometry optimizations of the four possible arrangements of water relative to $HCOO^-$ were carried out, and the binding energies of these complexes relative to isolated $HCOO^-$ + HOH are indicated alongside the corresponding arrows in Figure 1. It should be especially noted that when optimized, the T–C structure rearranges somewhat to form the C_{2v} geometry illustrated in the upper right corner of Figure 1, which contains two equivalent but distorted H bonds. This structure is denoted T–Cyc to indicate its cyclic nature.

Table III. Optimized Geometries (Å and deg) of Various Configurations of $(HCOO\cdots HOH)^-$ and Related Energetics (kcal/mol)[a]

	T–Cyc	T–T	C–T	C–C
$R(O^a\cdots O^b)$	2.924	2.772	2.757	2.784
$r(O^bH^a)$	0.957	0.968	0.969	0.969
$r(CO^a)$	1.235	1.241	1.242	1.240
$r(CO^c)$	1.235	1.226	1.226	1.225
$r(CH^c)$	1.109	1.111	1.111	1.115
$r(O^bH^b)$	0.957	0.947	0.947	0.947
δ	27.1	15.9	10.5	6.9
α	92.9	144.9	145.1	124.2
$\theta(H^aO^bH^b)$	99.0	102.6	103.2	104.0
$\theta(H^cCO^a)$	115.3	114.3	114.7	114.6
$\theta(H^cCO^c)$	115.3	115.7	115.6	115.3
E^{SCF}	0.0[b]	3.0	2.8	3.5
E^{MP2}	0.0[c]	3.7	3.4	3.8
$E_d^{SCF,d}$	15.4	13.0	13.2	12.7
$E_d^{MP2,d}$	17.4	14.7	15.0	14.6

[a] See Figure 2 for atomic labeling scheme. All complexes are planar. [b] E^{SCF} = −264.01092. [c] E^{MP2} = −264.72097. [d] Dissociation energy of each complex to $HCOO^-$ + HOH, including SCF zero-point vibrational energies.

(17) Scheiner, S. *J. Chem. Phys.* **1981**, *75*, 5791.

Table IV. Salient Features of Optimized Geometries (Å and deg) and Relative SCF Energies (kcal/mol) Obtained for $R(O^a\cdots O^b)$ = 2.8 Å.

	T-T			C-T			C-C		
	OCOH···O	OCO·H·O	OCO···HO	OCOH···O	OCO·H·O	OCO···HO	OCOH···O	OCO·H·O	OCO···HO
$r(O^aH^a)$	1.037	1.256	1.889	1.013	1.287	1.856	1.015	1.284	1.841
$r(H^aO^b)$	1.769	1.547	0.967	1.802	1.514	0.968	1.788	1.517	0.970
$\theta(CO^aH^a)$	117.7	118.7	137.1	108.7	111.4	139.4	109.8	112.2	127.8
$\theta(CO^aO^b)$	122.4	121.6	145.2	101.0	110.5	144.9	106.0	111.3	124.2
$\theta(O^aO^bH^a)$	2.8	2.4	15.9	−4.3	−0.9	10.5	2.2	0.8	7.0
E	33.8	36.8	0.2	27.1	32.9	0[a]	28.4	34.0	0.7

[a] E^{SCF} = −264.006 38 au.

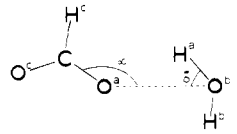

Figure 2. Atomic labeling scheme used for $(HCOO\cdots HOH)^-$. Structure shown is the C-T geometry. δ is defined so as to be positive when H^a and H^b lie on opposite sides of the $O^a\cdots O^b$ axis. All atoms are coplanar.

The details of the geometry of this structure are reported in Table III along with those of the other three configurations. The atomic labeling scheme used here and throughout this paper is presented in Figure 2. Because of the importance of these two angles and for purposes of consistency with prior work, $\theta(CO^aO^b)$ and $\theta(O^aO^bH^a)$ are frequently abbreviated as α and δ, respectively, as indicated in the figure.

The most stable of the various complexes is the T-Cyc arrangement, consistent with previous calculations using differing basis sets.[18] This structure owes its stability in part to the presence of two H bonds, albeit bent ones, rather than the single bond of each of the other structures, Another important factor is the optimal alignment of the HOH dipole moment, pointing directly toward the center of negative charge of $HCOO^-$ in the C_{2v} geometry. Along this vein, it may be noted that the $H^aO^bH^b$ angle is only 99° in the T-Cyc geometry, several degrees smaller than in the other complexes and fully 8° less than in isolated HOH. The energetic cost of this angular distortion is apparently repaid by the better ion–dipole interaction in the complex, resulting from the larger dipole moment of water (2.44 D for θ = 99.0° vs 2.29 D for θ = 106.6°).[19] In another sense, the angle reduction allows the two water hydrogens, with their partial positive charges, to better position themselves between $HCOO^-$ and O^b with its partial negative charge,

The $R(O^a\cdots O^b)$ distances of the three "open" complexes incorporating a single H bond are all quite close to one another, as are most of the other features of their geometries and energies.[20] The H bonding between water and O^a pulls the bridging proton (H^a) further away from O^b as well as producing a stretch in the CO^a bond, In all cases, the angle δ takes a positive value, which allows the positive end of the HOH dipole moment to turn a bit toward the proton-accepting O^a atom on which resides a substantial negative charge. The deviation of the bridging proton from the $O^a\cdots O^b$ axis is smallest (7°) in the C-C geometry and grows to as large as 16° in T-T,

Perhaps the most significant difference between these three open structures involves the angle α. Whereas α is equal to 145° for the T-T and C-T complexes, the smaller value of 124° is observed in C-C. The large angles in the former cases arise from the pivoting of the HOH subunit around H^a, which turns its dipole moment toward the partial negative charge[21] of O^a. Because of its different orientation in the C-C configuration, the water is required to rotate in the opposite direction, i.e. toward a smaller value of α, in order to achieve a similar alignment.

The cyclic structure in the first column of Table III of course exhibits some fundamental differences from the three open geometries. The two H bonds in the cyclic structure are substantially distorted from an optimal arrangement with the protons deviating from the O···O axes by 27°. This distortion is diminished somewhat by the reduction of the internal θ(HOH) angle in water, which also raises its dipole moment, as mentioned above. Adding to the angular strain on the H bonds, the α(CO···O) angles are only 93°, in comparison to the larger values between 124° and 145° in the open complexes. The two O···O axes in the cyclic structure are also substantially longer than the single H bond in each of the open structures. In line with the weaker H bonds in T-Cyc, the OH bonds of HOH are stretched by a lesser amount (0.01 Å) as compared to the H-bonding protons in the open complexes (0.02 Å).

The last several rows of Table III contain the relative energies of the various complexes and their binding energies, E_d, relative to the isolated subunits $HCOO^-$ and HOH. The latter quantity has been corrected for zero-point vibrational energies. It is significant that while inclusion of electron correlation increases the binding energy of each complex by some 2 kcal/mol, it does not influence the relative stabilities of the four geometries, as may be noted by comparison of the E^{SCF} and E^{MP2} rows of Table III. Another point worthy of note is that the binding energy of the anionic $(HCOO\cdot H\cdot OH)^-$ system is roughly only half that calculated earlier[7] for the cationic $(HC(OH)O\cdot H\cdot OH_2)^+$ analogue. Consistent with this weaker binding is the longer H-bond length: R(O···O) averages 2.77 Å for the anion and 2.55 Å for the cation.

Due to the substantially higher proton affinity of OH^- as compared to $HCOO^-$, a difference of some 50 kcal/mol, there are no stable minima found of the type $(HCOOH\cdots OH)^-$ in our calculations,

IV. Dependence upon Length of H Bond

When the H bond occurs as an intramolecular interaction within a macromolecule such as a protein, the geometry of the bond is controlled in large measure by the structural restraints imposed upon it by the entire system. As has been done in the past,[4-7] this phenomenon is modeled in our calculations by choosing a particular value of the H-bond length $R(O^a\cdots O^b)$ and holding this distance fixed as the proton transfers from one group to the other; all other geometrical parameters are fully optimized at each stage of the proton transfer. The transfer potential generated in this fashion represents a slice through the full potential energy surface of the system. While there are no minima in the full surface corresponding to $(HCOOH\cdots OH)^-$, a structure of this type may appear as a minimum within such a slice.[5] That is, when $R(O^a\cdots O^b)$ is held fixed, the potential energy profile takes a dou-

(18) (a) Gao, J.; Garner, D. S.; Jorgensen, W. L. *J. Am. Chem. Soc.* **1986**, *108*, 4784. (b) Berthod, H.; Pullman, A. *J. Comput. Chem.* **1981**, *2*, 87. (c) Lukovits, I.; Karpfen, A.; Lischka, H.; Schuster, P. *Chem. Phys. Lett.* **1979**, *63*, 151. (d) Alagona, G.; Ghio, C.; Kollman, P. *J. Am. Chem. Soc.* **1983**, *105*, 5226.

(19) Calculated for HOH with 4-31+G* basis set at SCF level; r(OH) = 0.948 Å for θ = 106.6°, the fully optimized geometry of water, and 0.9565 Å for θ = 99.0°, the geometry optimized within the complex.

(20) The geometries of all three open complexes were optimized with somewhat tighter convergence criteria than the normal default values. Criteria used are as follows: max force, 1.5×10^{-5}; RMS force, 1.0×10^{-5}; max displacement, 6.0×10^{-5}; RMS displacement, 4.0×10^{-5}. These values are 30 times smaller than default values. Although the gradient optimization procedures identified all three open complexes as minima, calculations involving analytical second derivatives indicated the Hessian matrix of the C-C complex contains a slightly negative eigenvalue (−0.0008 au). The corresponding eigenvector consists primarily of out-of-plane motion of the water. It should be noted that the C-C arrangement has been predicted as a minimum in a number of previous ab initio calculations as well.[18]

(21) The Mulliken charge of the carbonyl oxygen of trans HCOOH is −0.58e.

ble-well shape in which an energy barrier separates the (HCO-OH···OH)$^-$ and (HCOO···HOH)$^-$ configurations.

The key geometrical parameters of the two minima in the potential, as well as the transition state separating them, are presented in Table IV for $R(O^a\cdots O^b)$ = 2.8 Å. Our shorthand notation omits the nonbridging protons; hence, OCOH···O and OCO···HO represent the (HCOOH···OH)$^-$ and (HCOO···HOH)$^-$ minima, respectively, while OCO·H·O refers to the transition state separating them. In all cases, as the proton shifts to the left toward O^a, the $\theta(CO^aH^a)$ angle becomes smaller. In both the C–T and C–C cases, this angle is 109–110° in the OCOH···O configuration, slightly smaller than in the isolated HCOOH subunit. In contrast, the same angle is significantly larger, 117.7°, for T–T. The key to understanding this difference resides in the interaction between the OH$^-$ anion left behind by the departing proton and the atom of HCOOH to which OH$^-$ is closest (excepting the H-bonding atoms), viz. either H^c or O^c. In both C–T and C–C, the first C letter indicates the OH$^-$ anion is cis to H^c, whereas its trans arrangement in T–T places it in proximity to O^c. The partial negative charge of the latter atom[21] repels OH$^-$, resulting in the large value of $\theta(CO^aO^b)$ in the T–T OCOH···O structure (cf. C–T and C–C). This displacement of OH$^-$ pulls the bridging H^a atom along with it to some extent, explaining the large value of $\theta(CO^aH^a)$. The small values of $\theta(O^aO^bH^a)$ indicate the bridging proton lies very nearly along the H-bond axis for all but the OCO···HO configuration.

The last line of Table IV contains the relative SCF energies of the various configurations. In all three cases, the OCO···HO configuration is notably more stable than the OCOH···O geometry, again consistent with the considerably higher proton affinity of OH$^-$ as compared to HCOO$^-$. When we focus in on specifics, the OCOH···O configuration of the T–T geometry is 33.6 kcal/mol higher in energy than the OCO···HO structure, as compared to differences of only 27 kcal/mol for C–T and C–C. The high energy of the T–T OCOH···O configuration is due chiefly to the aforementioned repulsion between the OH$^-$ anion and the partial negative charge of the carbonyl oxygen of HCOOH, the same factor that enlarges the $\theta(CO^aO^b)$ angle in that structure.

In all three cases, the transition state OCO·H·O is only a few kilocalories higher in energy than OCOH···O, corresponding to a low barrier for transfer of a proton from HCOO$^-$ to OH$^-$. The barriers for the C–T and C–C configurations are nearly equal, ca. 6 kcal/mol, and somewhat higher than that in the T–T case (3 kcal/mol). The barrier reduction in the latter case is due to the destabilization of the OCOH···O configuration arising from the repulsion between OH$^-$ and O^c.

In addition to a H-bond length of 2.8 Å, transfer potentials were calculated for longer distances as well. In each case, all geometrical parameters were fully optimized with the exception of $R(O^a\cdots O^b)$. The lower group of curves in Figure 3 illustrates that the barrier for transfer of a proton from HCOO$^-$ to OH$^-$ (designated OCOH→O) rises as the H-bond is elongated.[22] Note that the three curves are approximately parallel, indicating nearly identical dependence upon R of the T–T, C–C, and C–T geometries. The lower barrier noted above for the T–T arrangement when R = 2.8 Å carries over to longer distances as well; the T–T curve is uniformly lower than the other two.

Because of the much greater stability of the OCO···HO configuration, the barrier for transfer in the reverse direction, OCO ← HO, is considerably higher, as illustrated by the upper set of curves in Figure 3. Nevertheless, these barriers exhibit a rapid rise with increasing R, quite akin to the forward OCOH → O barriers. The near equality of barriers for the C–T and C–C geometries is again evident for the OCO ← HO direction of transfer.

Since the T–Cyc geometry contains the best alignment of the HOH dipole with the HCOO$^-$ charge, it will clearly be most stable

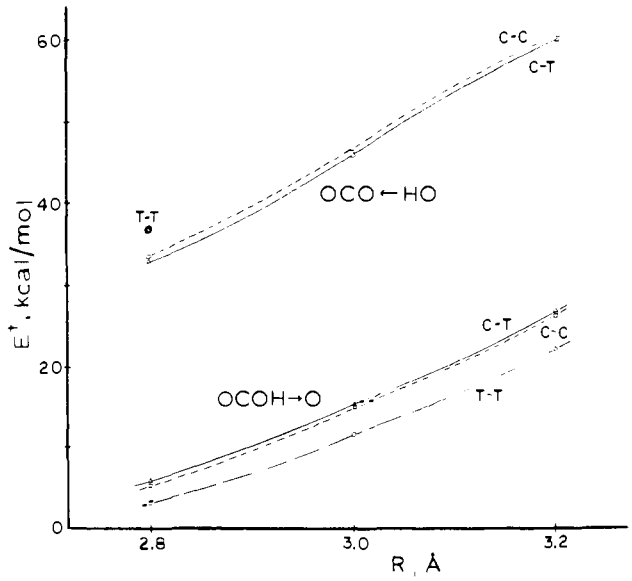

Figure 3. Energy barriers computed at various values of $R(O^a\cdots O^b)$. OCOH → O refers to transfer from HCOO$^-$ to OH$^-$, while the reverse direction is indicated by OCO ← HO. No barriers are provided for the latter direction of transfer in the T–T structure for $R > 2.8$ Å since the (HCOO···HOH)$^-$ geometry rearranges to T–Cyc beyond this intermolecular separation.

for long separation where this electrostatic interaction dominates. It is therefore not surprising to observe rearrangement of the T–T geometry of OCO···HO to T–Cyc at large R since such a conversion requires only relatively small reorientation of the two subunits. Specifically, optimization of the T–T geometry of the OCO···HO configuration, for $O^a\cdots O^b$ distances in excess of 2.8 Å, led to rearrangement to a T–Cyc type of cyclic structure. Without a OCO···HO minimum, it is hence not possible to determine OCO ← HO transfer barriers for the T–T structure for $R > 2.8$ Å. In fact, it is the marked propensity for rearrangement that accompanies proton transfer within the T–Cyc type of geometry that makes it impossible to study this structure without complications involving large-scale reorientations.

We note finally that previous calculations[5,23] have shown that inclusion of electron correlation typically stabilizes preferentially the transition state of the proton-transfer process, thereby lowering the barrier. The (HCOO·H·OH)$^-$ system is no exception in this regard. When MP2 theory is applied to the stationary points previously optimized at the SCF level in the T–T and C–T potentials for R = 2.8 Å, the OCO·H·O transition state is stabilized more than are the OCOH···O and OCO···HO minima. A more detailed search of the entire correlated surface would be required to determine whether the shallow barrier separating the two minima in the SCF potential is retained in the MP2 potential as well; such calculations are beyond our present computational resources. It is nonetheless clear that the transfer barriers in Figure 3 would be lowered by inclusion of electron correlation, consistent with earlier work, while enlargement of the basis set may be expected to increase these barriers somewhat.

V. Angular Distortions

Previous calculations[4-7] have examined the effects of angular distortions upon the energetics of proton transfer. Of particular note, it was found that, in the $(H_2CO\cdot H\cdot OH_2)^+$ and (HC(OH)-O·H·$OH_2)^+$ systems, a motion that increases the intermolecular C–O···O angle between the carbonyl or carboxyl group and a proton-accepting water molecule shifts the equilibrium position of the bridging proton away from the C–O and toward the water.[6,7] This trend was attributed to electrostatic interaction between the center of positive charge of the subunit on which the bridging

(22) At the present time, there is no clear rigorous relationship between energetic aspects of the proton-transfer potential and geometric features of the H bond. The curves in Figure 3 are thus merely intended to connect calculated points.

(23) Scheiner, S.; Szczesniak, M. M.; Bigham, L. D. *Int. J. Quantum Chem.* **1983**, *23*, 739. Szczesniak, M. M.; Scheiner, S. *J. Chem. Phys.* **1982**, *77*, 4586. Scheiner, S.; Harding, L. B. *J. Am. Chem. Soc.* **1981**, *103*, 2169.

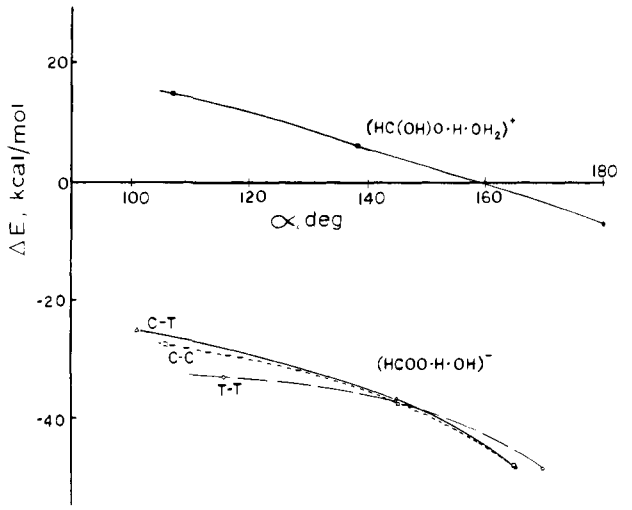

Figure 4. Calculated values of $\Delta E = E(\text{OCO}\cdots\text{HO}) - E(\text{OCOH}\cdots\text{O})$ for $(\text{HCOO}\cdot\text{H}\cdot\text{OH})^-$ and $(\text{HC(OH)O}\cdot\text{H}\cdot\text{OH}_2)^+$ as a function of α, the $\text{C}-\text{O}^a\cdots\text{O}^b$ angle. R is equal to 2.8 Å for the former system and 2.75 Å for the latter. The CC–C geometry of the cationic system is plotted (see ref 7 for explanation of nomenclature).

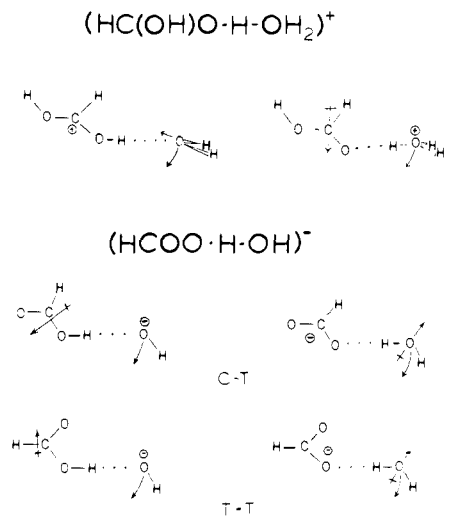

Figure 5. Schematic diagram of (OCOH···O) and (OCO···HO) configurations of $(\text{HC(OH)O}\cdot\text{H}\cdot\text{OH}_2)^+$ and $(\text{HCOO}\cdot\text{H}\cdot\text{OH})^-$. The former system is in its CC–C geometry.[7] Straight arrows represent approximate orientations of dipole moments of neutral subunits while curved arrows indicate the motion of the hydroxyl subunit associated with an increase in the α angle.

proton resides and the dipole moment of the partner neutral subunit. The situation is somewhat different in the present anionic $(\text{HCOO}\cdot\text{H}\cdot\text{OH})^-$ case since association with the central proton produces a neutral while it is the unprotonated partner subunit that remains (negatively) charged. This crucial distinction, coupled with the potential importance of the angular effects on proton position, warranted an inquiry into the differences in behavior between the cationic and anionic systems.

Consistent with earlier work, after first fixing the $R(\text{O}^a\cdots\text{O}^b)$ distance to 2.8 Å, a series of different values was chosen for the α angle describing $\theta(\text{C}-\text{O}^a\cdots\text{O}^b)$. The proton-transfer potential was then computed by optimizing all other geometrical parameters at each stage of transfer. As before, the difference in energy between the two configurations is defined as $\Delta E = E(\text{OCO}\cdots\text{HO}) - E(\text{OCOH}\cdots\text{O})$. The results are presented in the lower portion of Figure 4 for each of the three geometries of the anionic system discussed above.

The first point to be emphasized is that, in all three cases, ΔE becomes more negative as the α angle approaches 180°. This trend mimics what was seen earlier[7] in the cationic $(\text{HC(OH)O}\cdot\text{H}\cdot\text{OH}_2)^+$ system despite the reversal in charge. As a matter of fact, comparison with the relevant data for the latter cationic system, also plotted in Figure 4, shows a surprising degree of quantitative similarity.

To aid in understanding this behavior, the relevant configurations of the cationic and anionic systems have been illustrated schematically in Figure 5. All structures have been sketched for a C–O···O angle of about 120°, allowing a nearly linear O–H···O arrangement in the OCOH···O configuration. Let us first compare the C–T geometry of $(\text{HCOO}\cdot\text{H}\cdot\text{OH})^-$ with the structure of $(\text{HC(OH)O}\cdot\text{H}\cdot\text{OH}_2)^+$ directly above it in the figure. The specific structures considered are such that, in either case, the proton-accepting hydroxyl group is in proximity to the C–H bond of HCOOH (rather than the C–O bond). For each configuration, the charged subunit is indicated by the appropriate circled + or − sign while the dipole moment of the neutral subunit is represented by an arrow. (The directions and magnitudes of these moments were calculated with the 4-31+G* basis set.)[24]

Considering first the OCOH···O configurations on the left of Figure 5, we see a favorable linear H bond in which the bridging proton lies along the O···O axis, Increases in the C–O···O angle are indicated in the figure by the small downward curved arrows showing the motion of the pertinent O atom. Such a motion will distort the H-bond linearity, thereby raising the energy of either system. However, there is a distinct difference between the cationic and anionic systems. The dipole moment of the OH_2 in the upper left diagram points toward the center of positive charge of $HC(OH)_2^+$; increasing α will not alter this favorable alignment significantly. In contrast, the same motion of the OH^- in the left diagram immediately below will take it away from the positive end of the HCOOH moment, adding an electrostatic component to the distortion energy. A simple calculation of the ion–dipole term suggests this component may be as much as 15 kcal/mol when α changes from 120° to 180°. In fact, increasing α toward 180° does produce a markedly higher increase in the total energy of the anionic OCOH···O configuration than in the cation.

Let us turn now to the OCO···HO configurations on the right side of Figure 5. In the cationic case, the dipole moment of the HCOOH does not point toward the H_3O^+ ion in the upper diagram. Increasing α will produce the indicated motion of this cation, which will take it toward the negative end of the HCOOH dipole. It is hence not surprising that our calculations reveal a lower total energy as α approaches 180°. In the anion case, on the other hand, a similar motion of the neutral OH_2 subunit in the pertinent diagram on the right will have little influence upon its orientation with respect to the $HCOO^-$ center of charge. Indeed, the calculated energy of this configuration was found to be quite insensitive to changes in α.

When these trends are summarized for the cationic system, the OCOH···O configuration is raised in energy by the increase in α toward 180° while the OCO···HO configuration is stabilized. These two factors combine to yield a more negative value of ΔE for larger angles α. The OCOH···O configuration of the anion is also raised in energy as α increases, somewhat more so than the cation. However, since the OCO···HO configuration of the anion is little affected by changes in α, the net result is that ΔE in the anion decreases at approximately the same rate as that in the cation as α rises toward 180°.

It may be noted in Figure 4 that the curve for the C–C geometry is nearly coincident with the C–T curve. The switch from C–T to C–C corresponds to reversing the OH^- hydrogen in the C–T diagram on the left of Figure 5 from a downward position to one in which it is pointing upward. Since such a switch would have little effect on the overall negative charge of OH^-, it would not be expected to alter the dependence of the energy upon α. This is indeed borne out by the calculations. Similar repositioning of this hydrogen in the right C–T diagram would alter the direction of the HOH dipole moment. Nevertheless, the energy of the $(\text{HCOO}\cdots\text{HOH})^-$ configuration retains its low sensitivity to α.

(24) The calculated magnitudes of the dipole moment of HCOOH are the following: T, 1.71 D; C, 4.60 D. The angle between the dipole vector and the C=O bond is 21.0° in the trans structure and 16.3° in cis.

Hence, the energy of neither the OCOH···O nor the OCO···HO configuration is much affected by the switch from C–T to C–C, leading to the approximately coincident curves in Figure 4.

In contrast, the T–T curve in the figure is noticeably less steep than are the other two. This discrepancy is not associated with the $(HCOO\cdots HOH)^-$ configuration, the energy of which is again quite insensitive to changes in α. The reason for this insensitivity is clear in the diagrams on the right of Figure 5, which illustrate the change from C–T to T–T produces a small motion of the center of negative charge in $HCOO^-$ relative to the other subunit but no other real alterations. On the other hand, $(HCOOH\cdots OH)^-$ is substantially changed in that the HCOOH molecule is not longer in its cis configuration, but instead the two hydrogen atoms are now trans to one another. The dipole moment of the T structure of HCOOH is quite a bit smaller than that of the C geometry,[24] indicated by the smaller arrow in Figure 5. In addition, the direction of the moment has changed to the point where its interaction with the charge of OH^- in the T–T geometry is quite small when α is about 120° or so. A simple calculation indicates the ion–dipole term is perhaps 20 kcal/mol less attractive for T–T than for C–T at this angle. It is this higher energy of the OCOH···O configuration that is responsible for the more negative values of ΔE for the T–T structure in the small α regime.

As note above for C–T, increasing α takes the OH^- ion away from the positive end of the moment. This produces a lowering of the ion–dipole attraction by about 15 kcal/mol. In contrast, the lower left diagram in Figure 5 illustrates that the same motion in T–T brings the OH^- *toward* the positive end of the HCOOH moment. Thus, as α increases toward 180°, there is an increased ion–dipole stabilization (computed to be on the order of 4 kcal/mol), which partially compensates for the increasing nonlinearity of the O–H···O bond, causing the energy of the $(HCOOH\cdots OH)^-$ configuration to rise less quickly than that in the C–T case. This slower increase in energy results in the more gradual drop in ΔE as α approaches 180° in Figure 4.

While the curves in Figure 4 for the cationic and anionic systems are approximately parallel, it is obvious that the values of ΔE are uniformly much more positive for $(HC(OH)O\cdot H\cdot OH_2)^+$. This difference is related to the proton affinities of the pair of subunits in each system. Considering first the cationic system, the relevant subunits are the neutral HCOOH and OH_2 molecules. The proton affinity of the former is higher by some 13 kcal/mol than the latter.[7] Hence, the $(HC(OH)OH\cdots OH_2)^+$ configuration is more stable than $(HC(OH)O\cdots HOH_2)^+$ for small α, corresponding to positive ΔE. Yet the difference is small enough that increasing α can reverse the order of stability. The situation is quite different in the anionic $(HCOO\cdot H\cdot OH)^-$ system. The proton affinity of OH^- is very much larger than that of $HCOO^-$, a difference of some 50 kcal/mol. ΔE is thus quite negative at small values of α and only becomes more so as this angle is increased.

In summary, the trait that both the cationic and anionic systems share is that in either case displacement of the hydroxyl group toward the C–O axis (increasing α) favors the association of the bridging proton with the hydroxyl group. The similar rates at which ΔE becomes more negative as α increases in the two types of system is quite notable. The major difference is that the proton affinities of the subunits are such that the proton will normally prefer HCOOH to OH_2 whereas this trend is reversed in the anions since OH^- is very much more basic than $HCOO^-$.

Transfer Barriers. In addition to ΔE, the difference in energy between the two wells in the potential, we are also very much interested in the energy barrier separating the two wells since this property is directly related to the kinetics of the transfer process.[25] These barriers are presented in Figure 6 where the OCOH → O designation indicates transfer from carboxylate to hydroxide and the reverse direction is represented by OCO ← HO. Since $HCOO^-$ is 50 kcal/mol less basic than OH^-, the barriers blocking the transfer of a proton from the former to the latter are of course much smaller than the reverse OCO ← HO barriers.

It may first be noted that the barriers for proton transfer from

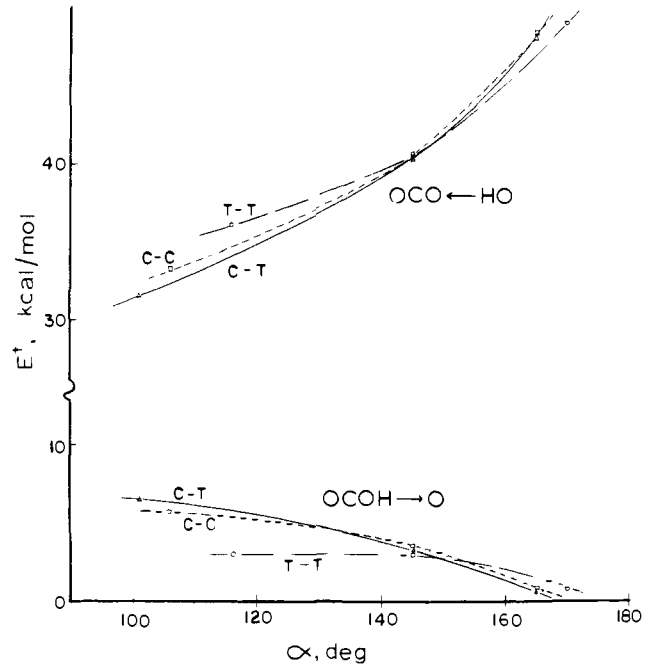

Figure 6. Energy barriers to proton transfer in $(HCOO\cdot H\cdot OH)^-$ for R = 2.8 Å. Transfer from $HCOO^-$ to OH^- is indicated by OCOH → O while OCO ← HO refers to reverse direction.

$HCOO^-$ to OH^- diminish as α increases toward 180° whereas the reverse barriers undergo an increase. This pattern is consistent with the trend of decreasing ΔE in Figure 4 in that both suggest a preferential stabilization of the right side of the potential for large α. Just as was observed for ΔE in Figure 4, the transfer barriers of the C–T and C–C geometries are nearly equal to one another. The T–T barriers diverge from these results to some extent, expecially at smaller values of α. The OCOH → O barriers vanish as α approaches 180°, indicating the collapse of the double-well potential into one with single-well character. (It is for this reason that the ΔE curves for $(HCOO\cdot H\cdot OH)^-$ in Figure 4 could not be extended all the way to 180°.)

One of the more curious features of Figure 6 is the leveling off of the T–T OCOH → O barriers for values of α less than 145° or so. This behavior is again rooted in the fact that the T–T $(HCOOH\cdots OH)^-$ configuration contains a neutral HCOOH molecule in which the two hydrogens are trans to one another while a cis HCOOH is associated with the C–T and C–C geometries. Due to the much smaller dipole moment of trans HCOOH as compared to that of cis,[24] the T–T $(HCOOH\cdots OH)^-$ configuration suffers from a diminished ion–dipole stabilization and hence tends to be higher in energy than the equivalent C–T and C–C configurations. At large values of α, the better alignment of the trans HCOOH dipole with the negative charge of OH^- can compensate for its smaller moment, but this is no longer true for small values of α. For example, the ion–dipole terms for the C–T and C–C OCOH···O configurations are nearly identical when α = 180° but differ by some 13 kcal/mol for α = 140°. The ensuing higher energy of the T–T $(HCOOH\cdots OH)^-$ configuration reduces the energy needed to climb to the top of the barrier, resulting in the flattening of the OCOH → O curve in Figure 6 as α is diminished.[26]

It is of particular interest to note relationships between geometrical parameters and energetic properties. Since the chief energetic expense of the transfer is associated with the stretching of the X–H bond (where X corresponds to the proton-donating atom), one might expect some correlation to exist between the proton-transfer barrier and the stretching of this bond in the transition state. Specifically, Δr is defined as the difference

(25) Scheiner, S.; Latajka, Z. *J. Phys. Chem.* **1987**, *91*, 724.

(26) For values of α smaller than about 115°, the water molecule in the T–T $(HCOO\cdots HOH)^-$ configuration rotates so as to resemble more closely the T–Cyc structure.

Table V. Changes in Energetics of Proton-Transfer Potential (kcal/mol) Caused by Motion of Hydroxyl Oxygen 40° out of the HCOO Plane[a]

	$(HCOO\cdot H\cdot OH)^-$		$(HC(OH)O\cdot H\cdot OH_2)^+$:
	$\alpha = 101°$	$\alpha = 165°$	$\alpha = 180°$
δE(OCOH···O)	4.0	−6.3	0.3
δE(OCO·H·O)	3.1	−5.5	−1.6
δE(OCO···HO)	−0.1	0.2	1.2
$\delta(\Delta E)$	−4.1	6.6	0.9
$\delta E^{\dagger}$(OCOH → O)	−0.9	0.9	−1.9
$\delta E^{\dagger}$(OCO ← HO)	3.2	−5.7	−2.8

[a] The C–T conformation of the anion is considered with R(OO) = 2.8 Å; the cationic geometry is CT–C with R = 2.75 Å.[7]

between r(X–H) in the geometries corresponding to the transition state and to the minimum of the potential. A very nearly linear relationship was indeed found between Δr and the energy barriers, $E^{\dagger}$. In the case of the OCOH → O barriers illustrated in the lower portion of Figure 6, the correlation coefficient is equal to 0.985; the analogous quantity for the reverse OCO ← HO direction is 0.987.

Out-of-Plane Deformations. Our previous study[7] of $(HC(OH)O\cdot H\cdot OH_2)^+$, the cationic analogue of the present system, revealed that pulling the hydroxyl oxygen atom out of the plane of the carboxyl group destabilizes the $(HC(OH)O\cdots HOH_2)^+$ configuration somewhat more than it does $(HC(OH)OH\cdots OH_2)^+$. The net result is that this deformation favors association of the bridging proton with the carboxyl at the expense of the hydroxyl group. Distortions of a similar type were imposed upon the anionic $(HCOO\cdot H\cdot OH)^-$ system, and the results are presented in Table V along with the previous data for $(HC(OH)O\cdot H\cdot OH_2)^+$. Specifically, the hydroxyl oxygen O^b was first placed in the HCOO plane at some distance R from O^a with the C–O^a–O^b angle defined as α. O^b was then displaced out of the HCOO plane by 40°, holding R and α fixed. The remainder of the geometrical parameters were fully optimized so as to locate the two minima in the potential, denoted OCOH···O and OCO···HO, and the transition state separating them, OCO·H·O. The values of δE in the first three rows of Table V correspond to the change in energy of each of these configurations relative to the case where O^b was left in the HCOO plane.

It may be noted from the first row of the table that the out-of-plane distortion causes a substantial change in the energy of the left well of the $(HCOOH\cdots OH)^-$ anion while that of the cation is nearly unperturbed. It is especially interesting that the 101° and 165° cases of the anion differ in the sign of this energy change. The situation reverses for the right wells in that the anion's energy is little affected by the out-of-plane deformation, in contrast to a larger change for the $(HC(OH)O\cdots HOH_2)^+$ cation.

In order to understand these deformation energies, let us take as our starting point the OCOH···O configuration with α = 101°. The H bond in this geometry is very nearly linear, i.e. $\theta(O^aH^aO^b) \cong 180°$. Perhaps even more important, the negative charge of the OH^- species is well aligned with the positive end of the very sizable dipole moment of HCOOH in its cis conformer.[24] Displacement of the OH^- out of the HCOOH plane therefore causes a destabilization of the system. In the case where $\alpha(CO^aO^b)$ = 165°, on the other hand, the OH^- lies far from (i) its optimal position for H bonding with HCOOH and (ii) the positive end of the HCOOH dipole moment vector. Hence, the out-of-plane displacement costs little and, in fact, leads to a net stabilization.[27] Due to the very negative value of ΔE for the proton-transfer reaction in the anion, Hammond's postulate[28] stipulates that the transition state is very similar in character to the left well $(HCOOH\cdots OH)^-$. The distortion energies for the OCO·H·O configuration are thus very much like those in the preceding row. In the OCO···HO configuration is little affected by the O^b displacement since the water molecule is free to rotate so as to maintain a nearly linear $O^a\cdots H^aO^b$ arrangement.

Comparison of the behavior of the anionic $(HCOO\cdot H\cdot OH)^-$ system with the cationic analogue[7] provides some instructive insights into the fundamental nature of the transfer process. In contrast to $(HCOO\cdot H\cdot OH)^-$ where the OCOH···O configuration is appreciably changed in energy by the out-of-plane deformation while OCO···HO is little affected, the deformation energies of $(HC(OH)O\cdot H\cdot OH_2)^+$ follow an opposite pattern wherein it is the latter configuration that is more strongly influenced. This behavior may be easily understood on the basis of an electrostatic model, which focuses on the interaction between the dipole moment of the neutral subunit and the charge of the ionic component.

Consider for example the OCOH···O configuration of the two systems. Within the context of the anionic $(HCOOH\cdots OH)^-$, the left subunit is a neutral HCOOH while the right subunit consists of a OH^- anion. Displacement of the hydroxyl oxygen from the HCOOH plane takes the anion away from the dipole moment of HCOOH (α = 101°), causing a substantial destabilization. (This does not occur for α = 165° since there is poor alignment to begin with.) The situation is quite different in the cationic $(HC(OH)OH\cdots OH_2)^+$ case where the left subunit is now charged (a cation) and the right subunit is a neutral OH_2 molecule. The dipole moment of the latter subunit is free to rotate around, continuing to point toward the center of positive charge of $HC(OH)_2^+$, as the hydroxyl is removed from the HCOO plane; hence, the corresponding deformation energy is rather small.

This scenario is reversed in the OCO···HO configurations. In the anion case, the left subunit is negatively charged while the right subunit is a neutral water. It is not very costly energetically to remove the water from the $HCOO^-$ plane since this deformation does not disrupt the ability of the water to rotate as needed; hence δE(OCO···HO) is rather small for $(HCOO\cdot H\cdot OH)^-$. This term is much larger for $(HC(OH)O\cdot H\cdot OH_2)^+$ because the left subunit is a neutral HCOOH. Removing the right-hand $(HOH_2)^+$ subunit from the carboxyl plane takes the charge away from the direction of the HCOOH dipole moment.

The fourth row of Table V reflects the combined effect of the distortion energies of the two minima in the potential. Since δE(OCOH···O) is larger than δE(OCO···HO) for the anionic system with α = 101°, the left side of the potential is raised more than the right and thus ΔE becomes more negative. A positive value occurs for α = 165° since δE(OCOH···O) is negative in sign. In the case of the $(HC(OH)O\cdot H\cdot OH_2)^+$ system, $\delta(\Delta E)$ is also positive, but this is now due to the destabilization of the right well. In summary, an out-of-plane distortion of the type investigated here can favor association of the bridging proton with either the hydroxyl oxygen or carboxylate group in $(HCOO\cdot H\cdot OH)^-$, depending on α, whereas the carboxyl group is favored in the cationic analogue.

VI. Summary and Conclusions

The most stable configuration of the complex formed between $HCOO^-$ and HOH is a C_{2v} cyclic one containing two distorted H bonds. A number of "open" complexes, each containing a single H bond, represent local minima on the potential energy surface. These complexes are all bound with roughly half the binding energy of the proton-bound complex of neutral HCOOH with HOH. Because of the ca. 50 kcal/mol higher proton affinity of OH^- as compared to that of $HCOO^-$, the full potential energy surface contains no local minima corresponding to $(HCOO\text{-}H\cdots OH)^-$.

When the $HCOO^-$ and OH^- groups are held apart at some arbitrary distance, on the other hand, the proton-transfer potential contains two distinct minima, $(HCOOH\cdots OH)^-$ and $(HCO\text{-}O\cdots HOH)^-$, with an energy barrier separating them; the latter minimum is, of course, considerably more stable than the former. The barriers to proton transfer in either direction rise quickly as the two subunits are pulled further apart. In what appears to be a general rule, electron correlation preferentially stabilizes the

(27) The hydroxyl hydrogen of HCOOH rotates around the C–O bond so as to follow OH^- up out of the plane. This motion generates an out-of-plane component of the HCOOH moment with which the OH^- can favorably interact.

(28) Hammond, G. S, *J. Am. Chem. Soc.* **1955**, *77*, 334.

transition state over the minima, resulting in a reduction in the transfer barriers.

Earlier work involving the C=O group of neutral molecules like H_2CO and HCOOH had demonstrated that, as the proton acceptor molecule is moved toward the C=O axis, there is a marked propensity of the bridging proton to shift its equilibrium position away from the C=O and toward the acceptor. The calculations reported here have provided evidence that the anionic $-COO^-$ group is characterized by the same tendency. This similarity is perhaps surprising at first sight, given the very different character of the subunits in the $(HC(OH)O\cdot H\cdot OH_2)^+$ and $(HCOO\cdot H\cdot OH)^-$ systems. Nevertheless, analysis of the results reveals that the trends in both systems can be attributed in a straightforward manner to a single principle relating to the ion–dipole interactions within the configurations corresponding to the two minima in the potential.

Proton-transfer potentials were examined for a number of different relative orientations of the $HCOO^-$ and OH^- subunits, i.e. cis or trans. In all cases, it was possible to explain qualitatively the calculated differences in optimized geometries and in the potentials on the basis of interactions between the partial charges on individual atoms at various stages during the proton-transfer process.

A notable distinction between the properties of HCOOH and $HCOO^-$ arises when the proton acceptor is removed from the carboxyl plane. Whereas the nonplanar geometry favors association of the bridging proton with the neutral carboxyl group, either the hydroxide or carboxylate is favored in the anionic system, depending upon their relative orientation. Nonetheless, as above, this behavior is simply explained in either case on the basis of the interaction between the dipole moment of the neutral subunit and the charge of the other. That is, in $(HC(OH)O\cdot H\cdot OH_2)^+$ association of the bridging proton with either subunit yields a cation, e.g. $HC(OH)_2^+$, leaving the other subunit neutral. In contrast, association of the proton with either subunit in $(HCOO\cdot H\cdot OH)^-$ yields a *neutral*, e.g. HCOOH while the other subunit is charged.

It is important to consider the proton-transfer properties of the carboxyl group within the context of a larger molecule such as an enzyme. Considering as a first example a H bond between –COOH and water, the former species has a somewhat higher proton affinity, making it a more likely acceptor of a proton, all things being equal. However, other factors may influence this propensity, most notably the interaction of the H-bonded system with the remainder of the protein. In addition, we have illustrated previously[7] that the position of the bridging proton may be shifted toward the water if the latter group is located more nearly along the C–O axis. In the case of higher pH where both the carboxyl and water have been deprotonated and exist as $-COO^-$ and $-OH^-$ ions, the situation is different since the proton affinity of hydroxide is very much larger than that of carboxylate. Nonetheless, the results reported here have suggested that if the basicities of the two ions can be equalized to some extent by the protein environment, the equilibrium proton position can again be shifted from one subunit to the other by adjustments in the angular features of the H bond. Whereas the –COOH and $-COO^-$ species are consistent with regard to in-plane aspects of the geometry, out-of-plane distortions can produce different proton shifts in the two charge states.

Acknowledgment. We are grateful to Drs. I. J. Kurnig and R. B. Brenstein for performing some of the pilot calculations. Some of the computations were performed on the SIU Theoretical Chemistry Computer, funded in part by a grant from the Harris Corp., and others at the San Diego Supercomputer Center. This work was supported by grants from the National Institutes of Health (GM29391 and AM01059).

Registry No. $HCOO^-$, 71-47-6; OH_2, 7732-18-5.

The ArF^+ Cation. Is It Stable Enough To Be Isolated in a Salt?

Gernot Frenking,*[,†,‡,1a] Wolfram Koch,[†,1b] Carol A. Deakyne,[1c] Joel F. Liebman,*[,1d] and Neil Bartlett[1e]

Contribution from the Molecular Research Institute, 701 Welch Road, Palo Alto, California 94304, IBM Almaden Research Center, San Jose, California 95120, Air Force Geophysics Laboratory, Ionospheric Interactions Division, Hanscom AFB, Massachusetts 01731, Department of Chemistry, University of Maryland, Baltimore County Campus, Baltimore, Maryland 21228, and Department of Chemistry, University of California, Berkeley, California 94720. *Received May 11, 1988*

Abstract: Ab initio calculations at the MP4(SDTQ)/6-311G(2df,2pd)//MP2/6-31G(d,p) level of theory predict that the dissociation energy D_0 of ArF^+ in the $^1\Sigma^+$ ground state is 49 ± 3 kcal/mol. The stabilization energies of ArF^+ salt compounds with suitable counteranions are estimated. The best candidates to form stable argon salts appear to be $ArF^+AuF_6^-$ and $ArF^+SbF_6^-$.

Since the synthesis of the first noble gas salt compound in 1962,[2] numerous molecules of the "inert" elements have become accessible as chemical reagents.[3,4] However, while many neutral and ionic species containing a noble gas element are known in the gas phase, no salt or stable solution containing a noble gas lighter than krypton has ever been prepared. It has generally been concluded that the threshold of true chemical reactivity is reached with Kr.[4] The most promising candidate to break that barrier seems to be ArF^+, salts of which might be preparable. ArF^+ is unique among

[†] Present address: IBM Wissenschaftliches Zentrum, Tiergartenstrasse 15, D-6900 Heidelberg, West Germany.

[‡] Present address: Institut für Organische Chemie, Universität Marburg, D-3550 Marburg, West Germany.

(1) (a) Molecular Research Institute. (b) IBM Almaden Research Center. (c) Air force Geophysics Laboratory. (d) University of Maryland. (e) University of California.

(2) Bartlett, N. *Proc. Chem. Soc., London* **1962**, 218.

(3) (a) *Noble Gas Chemistry. A Bibliography*: 1962–1976; Hawkins, D. T., Falconer, W. E., Bartlett, N., Eds.; IFI/Plenum Press: New York, 1978. (b) Seppelt, K.; Lenz, D. *Prog. Inorg. Chem.* **1982**, *29*, 167. (c) Selig, H.; Holloway, J. H. *Top. Curr. Chem.* **1984**, *124*, 33.

(4) *Advanced Inorganic Chemistry*; Cotton, F. A., Wilkinson, G., Eds.; Wiley: New York, 1987.

0002-7863/89/1511-0031$01.50/0 © 1989 American Chemical Society